THE
PHYSICAL REVIEW

A journal of experimental and theoretical physics established by E. L. Nichols in 1893

SECOND SERIES, VOL. 122, NO. 3 MAY 1, 1961

Incoherent Microwave Radiation from a Plasma in a Magnetic Field*

JAY L. HIRSHFIELD AND SANBORN C. BROWN
Department of Physics and Research Laboratory of Electronics, Massachusetts Institute of Technology, Cambridge, Massachusetts
(Received December 23, 1960)

The microwave emission from a plasma in a magnetic field is calculated theoretically using Kirchhoff's radiation law for cases when characteristic waves do not couple within the plasma. Experimental observations of radiation temperatures and cyclotron radiation line breadth and shape are cited to illustrate applications of the theory to experiment.

I. PLASMA IN A MAGNETIC FIELD AS A THERMAL EMITTER

In the limiting cases that will be discussed here, Kirchhoff's radiation law can be used to determine the thermal power $P(\omega)$ per solid angle radiated from a plasma of surface area S in the radian frequency interval $d\omega$ about ω[1,2]:

$$P(\omega)d\omega = kT_r \frac{d\omega}{2\pi} \frac{S}{\lambda^2} A(\omega). \quad (1)$$

Here λ is the wavelength of the radiation *in vacuo*, k is Boltzmann's constant, T_r is the radiation temperature, and $A(\omega)$ is the absorptivity of an electromagnetic test wave launched from the position of the observer. That is, for a test wave of specified polarization with electric and magnetic field intensities $\mathbf{E}_i$ and $\mathbf{H}_i$,

$$A(\omega) = \int_V \mathrm{Re}(\mathbf{E}\cdot\boldsymbol{\sigma}\cdot\mathbf{E}^*)dV \Big/ \int_S \mathrm{Re}(\mathbf{E}_i\times\mathbf{H}_i^*)\cdot d\mathbf{S}, \quad (2)$$

where $\boldsymbol{\sigma}$ is the (tensor) rf conductivity of the plasma—a function of frequency and plasma composition—and $\mathbf{E}$ is the electric field within the plasma. Equation (1) also gives the net radiation flowing down a waveguide containing a plasma, provided that the S/λ^2 factor is set equal to unity.

In general, the numerator of Eq. (2) is a sum of terms, one for each characteristic wave within the plasma, with the components of E determined from a boundary-value solution for the plasma that is in question; terms in Eq. (2) for those characteristic waves that are different from the incident wave arise from coupling between waves.

In establishing Eq. (1) for a plasma in free space, the plasma must, in general, be homogeneous and of sufficient geometrical symmetry so that reciprocity is maintained for propagation to and from the observer. For a plasma in a waveguide, the symmetry condition can be relaxed so that Eq. (1) applies to inhomogeneous, irregularly shaped plasmas, provided that they have a plane of symmetry normal to the waveguide axis.

When the plasma is isotropic and homogeneous, the two individual polarizations can be treated separately and Eq. (1) can be written for either, or both, polarizations. However, since a plasma in a magnetic field is gyrotropic, the separate polarizations generally couple at the plasma boundary (or at gradients of refractive index within the plasma) and the full form of Eq. (2) is required. For a gyrotropic plasma in a waveguide, the complete set of vacuum modes is generally needed to satisfy boundary conditions at the plasma-vacuum interfaces.[3]

Solution of Eq. (1) for a plasma of arbitrary geometry and composition, therefore, is reduced to a boundary-value problem, with coupled polarizations (or modes), for determining the field $\mathbf{E}$ within the plasma. To avoid complexity, we consider cases in which this coupling is either absent or negligible. The coupling is absent for a homogeneous plane plasma slab with the external dc

* This research was supported in part by the U. S. Army Signal Corps, the Air Force Office of Scientific Research, and the Office of Naval Research; and in part by the U. S. Atomic Energy Commission.

[1] S. M. Rytov, *Theory of Electrical Fluctuations and Thermal Radiation* (Akademiia Nauk S. S. S. R., Moscow, 1953).

[2] F. V. Bunkin, Soviet Phys.—JETP **5**(32), 227 (1957); **5**(32), 655 (1957) (translation).

[3] P. S. Epstein, Revs. Modern Phys. **28**, 3 (1956).

magnetic field either parallel, or perpendicular, to the plasma boundaries. The coupling is negligible when the wave refractive indices in the plasma approach unity (that is, for a transparent plasma). The plasma will also be considered to be free of interference effects arising from neighboring boundaries; conditions under which this can be achieved have been discussed previously for plasmas without magnetic fields.[4]

Under these restrictions, a geometrical optics formalism is a good approximation for determining A; this can be shown to be equivalent to using the equations of radiative transfer,[5] one for each polarization or mode, in cases in which the equations are decoupled. As a result, we find that $A_n=(1-\Gamma_n)[1-\exp(-\tau_n)]$, where Γ_n is the power reflection coefficient at the plasma boundary and τ_n is the optical depth, both for the nth polarization (or mode). For a plasma of power absorption coefficient α_n, we have $\tau_n=\int_0^L \alpha_n(z)dz$, where L represents the plasma dimension.

The radiation temperature T_r in Eq. (1) has been determined for a steady-state, transparent plasma of arbitrary electron velocity distribution.[6] When the distribution of electron velocities is Maxwellian, T_r becomes T_e, the electron temperature. When collisions dominate the emission spectrum, $3kT_r/2$ becomes u, the average electron energy, whenever ν_c, the momentum-transfer collision frequency, is independent of electron velocity. Values of T_r for variations of ν_c with velocity and for various distribution functions have been found to deviate never more than 10% from the relation $3kT_r/2=u$ for helium (which was the gas used in our experiments).

II. CALCULATIONS OF THE EMISSION

This discussion will be divided into two parts distinguished by the magnitude of the absorption:

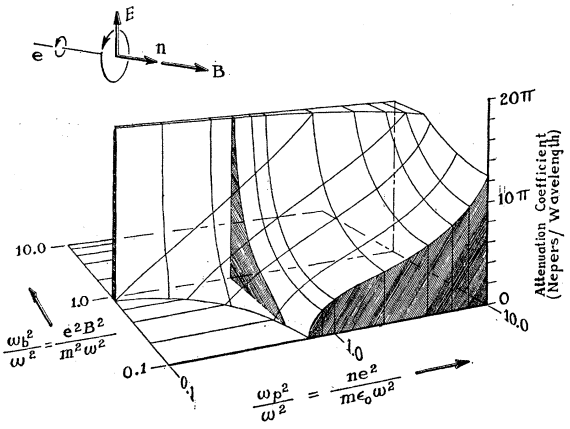

FIG. 1. Attenuation coefficient for the resonant wave propagating parallel to the magnetic field. No collisions.

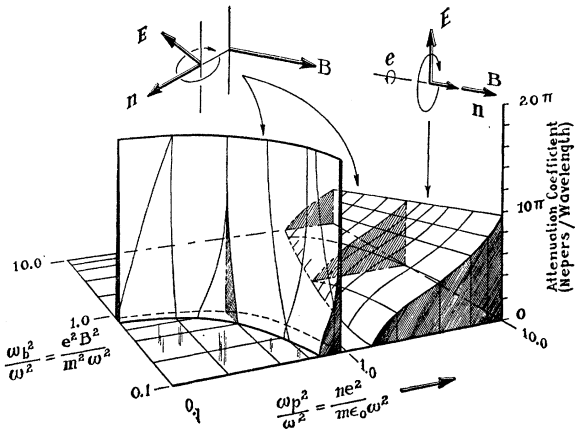

FIG. 2. Attenuation coefficient for the resonant wave propagating perpendicular to the magnetic field. No collisions.

$(\alpha\lambda/4\pi)\ll 1$, a weakly absorbing plasma; and $(\alpha\lambda/4\pi)\gtrsim 1$, a strongly absorbing plasma. We shall limit ourselves mainly to plasmas in which the electron's thermal motion has a negligible influence on wave absorption, although some effects of thermal motion in weakly absorbing plasmas will be treated.

Since the emission depends on the absorption through Kirchhoff's law, Eq. (1), we first summarize wave propagation and absorption in magnetoplasmas.

A. Absorption of Waves in a Plasma

Magneto-ionic wave theory for plasmas with negligible effects of electronic thermal motion dates from Appleton's ionospheric work.[7] Åström[8] and Allis[9] have reorganized the theory; we follow Allis' approach.

If we assume plane waves and infinitely heavy ions, Maxwell's equations yield a wave equation involving the elements of the tensor plasma dielectric coefficient which are obtained from the Boltzmann equation.[10] For no thermal motion, we obtain a biquadratic determinantal equation whose roots are the complex propagation constants as functions of radiation frequency, electron plasma frequency, electron cyclotron frequency, and collision frequency. The absorption coefficient follows from the imaginary part of the propagation constant.[11]

In Figs. 1 and 2 we have plotted the attenuation coefficient for waves propagating either parallel or perpendicular to the applied magnetic field; these are the angles of propagation to which our restrictions limit the eventual emission calculation for plasmas that are not transparent. The values shown in these figures are ob-

[4] G. Bekefi, J. L. Hirshfield, and S. C. Brown, Phys. Rev. **116**, 1051 (1959).
[5] D. F. Martyn, Proc. Roy. Soc. (London) **A193**, 44 (1948).
[6] G. Bekefi, J. L. Hirshfield, and S. C. Brown, Phys. Fluids (to be published).
[7] J. A. Ratcliffe, *The Magneto-Ionic Theory and Its Applications to the Ionosphere* (Cambridge University Press, New York, 1959).
[8] E. Åström, Arkiv Fysik **2**, 443 (1950).
[9] W. P. Allis and R. J. Papa, Quarterly Progress Report No. 55, Research Laboratory of Electronics, Massachusetts Institute of Technology, October 15, 1959 (unpublished), pp. 19–27.
[10] W. P. Allis, in *Handbuch der Physik*, edited by S. Flügge (Springer-Verlag, Berlin, 1956), Vol. 21, pp. 383–444.
[11] L. Mower, Technical Report No. MPL-1, Sylvania Electric Products, Inc., 1956 (unpublished).

tained in the limit of no collisions $(\nu_c/\omega)\rightarrow 0$, and therefore represent evanescent rather than dissipative attenuation. However, as we shall see, a small value of (ν_c/ω) will bring about dissipative attenuation that follows closely the calculation for $(\nu_c/\omega)=0$. The respective polarizations are indicated in both figures. We see the pronounced electron resonances given by $\omega=\omega_b$ for $\mathbf{n}\times\mathbf{B}=0$ (cyclotron resonance), and by $\omega=(\omega_b^2+\omega_p^2)^{\frac{1}{2}}$ for $\mathbf{n}\cdot\mathbf{B}=0$ (plasma resonance). Here $\mathbf{n}$ is the wave normal. The attenuation coefficient for $\mathbf{n}\cdot\mathbf{B}=0$ with polarization along $\mathbf{B}$ is not shown in Figs. 1 and 2; it is independent of magnetic field and follows the dependence on ω_p shown for the other waves when $\omega_p=0$.

The influence of a small value of (ν_c/ω) is shown in Figs. 3 and 4. Here are plotted the absorption coefficients, for the resonant wave, for θ, the angle between $\mathbf{B}$ and $\mathbf{n}$, equal to 0 and $\pi/2$, respectively. The curves are shown as functions of ω_b/ω with $(\omega_p/\omega)^2$ as a parameter. For $(\omega_p/\omega)^2\ll 1$ both cases are similar, each exhibiting a symmetrical resonance at $\omega=\omega_b$. As $(\omega_p/\omega)^2$ increases, the curves broaden toward lower values of (ω_b/ω) and the peaks in Fig. 4 move toward lower values of (ω_b/ω), following the relation $\omega=(\omega_b^2+\omega_p^2)^{\frac{1}{2}}$.

When $(\omega_p^2/\omega_b\nu_c)\ll 1$ so that the real part of the refractive index is essentially unity, the absorption coefficient for the resonant wave[12] is

$$\alpha\approx\frac{\omega_p^2}{c}\left(\frac{1+\cos^2\theta}{2}\right)\times\int_0^\infty f(v)\frac{d}{dv}\left[\frac{\nu_c}{\nu_c^2+(\omega-\omega_b)^2}\frac{4\pi v^3}{3}\right]dv, \quad (3)$$

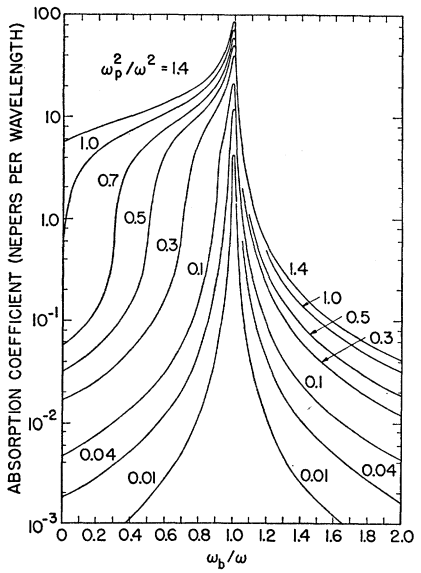

FIG. 3. Absorption coefficient for the resonant wave propagating parallel to the magnetic field. $(\nu_c/\omega)=10^{-2}$.

[12] L. Goldstein, in *Advances in Electronics and Electron Physics*, edited by L. Marton (Academic Press, Inc., New York, 1955), Vol. 7, pp. 399–503.

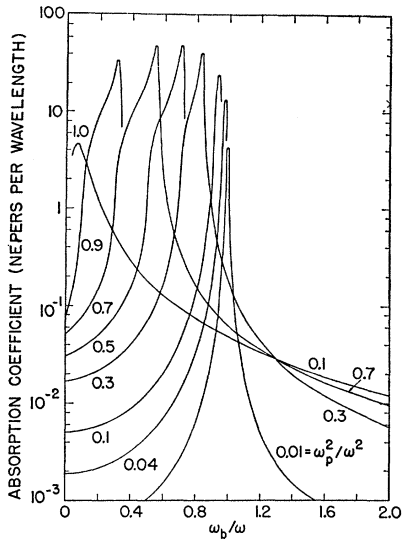

FIG. 4. Absorption coefficient for the resonant wave propagating perpendicular to the magnetic field. $(\nu_c/\omega)=7.5\times 10^{-3}$.

where the distribution of electron velocities $f(v)$ is normalized so that $\int_0^\infty 4\pi v^2 f(v)dv=1$. The nonresonant wave has an absorption coefficient that equals zero in this approximation. Equation (3) gives a Lorentz absorption profile,[13] typical of collision broadening.

Equation (3) shows the influence of the distribution of electron velocity on the absorption coefficient which arises from the velocity dependence of ν_c; otherwise it indicates that α is independent of $f(v)$. For the resonant waves, which are slow waves, the thermal electrons can move with the wave and therefore interact more strongly than is predicted for cold electrons.[14] One must now employ an absorption coefficient obtained by including electron thermal motion. For example, with $\nu_c=$ constant, $\theta=0$, and $f(v)=\exp[-(v/v_t)^2]$, we obtain[15]

$$\alpha\approx\frac{1}{\sqrt{\pi}}\frac{\omega_p^2}{\omega^2}\frac{\nu_c c}{v_t^2}\int_{-\infty}^{\infty}\exp(-y^2)dy\Big/\left[\left(\frac{\omega-\omega_b}{\omega}\frac{c}{v_t}-y\right)^2+\left(\frac{\nu_c}{\omega}\frac{c}{v_t}\right)^2\right], \quad (4)$$

where $(\omega_p^2/\omega_b\nu_c)\ll 1$, and $v_t^2=2kT/m$. Equation (4) gives a Voigt profile,[16] typical of a mixture of collision and Doppler broadenings.

[13] A. C. G. Mitchell and M. W. Zemansky, *Resonance Radiation and Excited Atoms* (Cambridge University Press, New York, 1934), Chap. IV.

[14] L. Mower, Phys. Rev. **116**, 16 (1959).

[15] J. L. Hirshfield, Quarterly Progress Report No. 58, Research Laboratory of Electronics, Massachusetts Institute of Technology, July 15, 1960 (unpublished), pp. 17–27.

[16] D. W. Posener, Australian J. Phys. **12**, 184 (1959).

B. Emission from a Weakly Absorbing Plasma (Cyclotron Radiation)

In this section, we calculate the cyclotron radiation from a weakly absorbing plasma from single-particle considerations, as has been done by Oster.[17] Comparison with the results of Sec. II-A will then show under what conditions these single-particle notions must be abandoned in favor of the complete approach through Kirchhoff's law.

When the emitting electrons of the plasma are sufficiently sparsely distributed that they radiate as if in vacuo, the power radiated per unit volume per unit solid angle[18] is

$$dP(v_\perp)=\frac{e^2\omega_b^2v^2dN(v_\perp)}{16\pi^2\epsilon_0c^3}\left(\frac{1+\cos^2\theta}{2}\right)\text{ watts/m}^3\text{ steradian},$$

where $dN(v_\perp)$ is the differential concentration of electrons having a component of velocity $v_\perp$ perpendicular to the magnetic field. When the emission is interrupted periodically by collisions of frequency ν_c that destroy phase coherence and with $v_\perp^2dN(v_\perp)=2\pi Nv^4dv\,\sin\phi d\phi$, the total power radiated per unit volume in a frequency interval $d\omega$ is[19]

$$P(\omega)d\omega=\frac{\omega_p^2\omega^2m}{6\pi^2c^2}\left(\frac{1+\cos^2\theta}{2}\right)\times\int_0^\infty\frac{\nu_cd\omega}{\nu_c^2+(\omega-\omega_b)^2}v^4f(v)dv\text{ watts/m steradian},\quad(6)$$

where the integration over ϕ has already been carried out.

This result is identical with that obtained from Eq. (4) with the use of Kirchhoff's law [Eq. (1)] for the resonant wave. That is, $P(\omega)d\omega=\alpha(\omega)B(\omega)$, with $B(\omega)=kT_r\omega^2d\omega/8\pi^3c^2$, if we substitute the value for T_r previously derived.[6]

Doppler broadening can be included in Eq. (6) by substituting $\omega_b[1-(v_z/c)\cos\theta]$ (using Cartesian velocity coordinates) for ω_b. For ν_c independent of electron velocity, we write $v^2=v_\perp^2+v_z^2$ and obtain the result given by Eq. (5) with the use of Kirchhoff's law.

Equation (6) and the discussion following it show that correct values for the cyclotron radiation, which is the reaction to radiation damping for free gyrating electrons, can be obtained from an absorption coefficient that is derived without consideration of radiation damping. This is seen to be reasonable by comparing the magnitudes of the radiation damping rate and the collision frequency, since for harmonic time dependence these two quantities can be combined. Their ratio is $\omega_b^2e^2/6\pi\epsilon_0mc^2\nu_c=6.25\times10^{24}\omega_b^2/\nu_c$, which is small compared with unity for cases of practical significance. Although it is an essential underlying mechanism, radiation damping does not influence the electron's acceleration, and thus does not directly enter into the absorption coefficient.

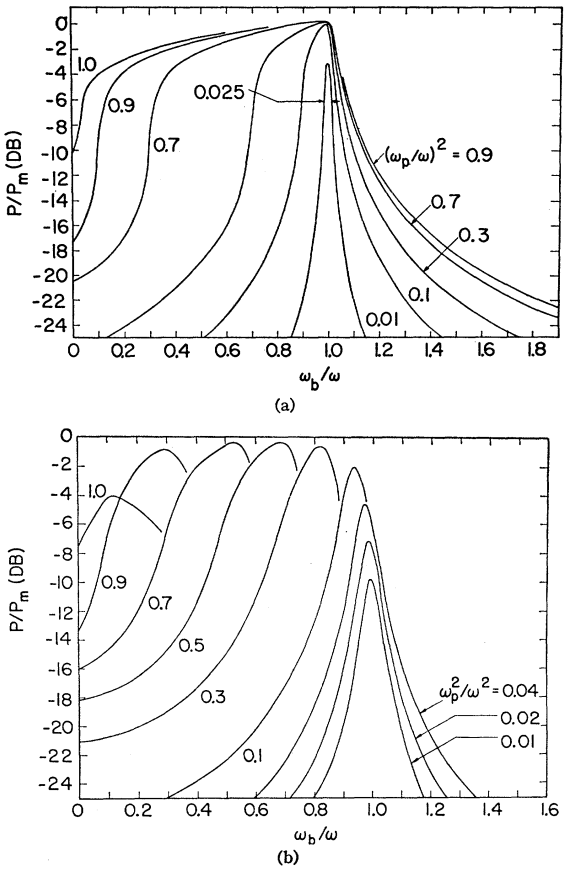

FIG. 5. Emission in two waves in a plasma: (a) Propagation parallel to the magnetic field, $(\nu_c/\omega)^2=10^{-4}$. (b) Propagation perpendicular to the magnetic field, $(\nu_c/\omega)^2=10^{-3}$.

For completeness Eq. (6) should contain a term identical to that shown, except that $-\omega_b$ is substituted for $+\omega_b$. This term arises from the nonresonant wave, with Kirchhoff's law used in computing the emission, or in the Fourier analysis of the interrupted radiation,[19] with the single-particle model used. When $(\nu_c/\omega_b)^2\ll1$, these additional terms are much smaller than the ones shown. They represent bremsstrahlung from binary encounters between electrons and heavy particles in the plasma.[4] The radiation from collisions, for a transparent plasma, is thus seen to be distinct from the cyclotron radiation (even though the collision frequency appears in expressions for cyclotron radiation) and of much smaller magnitude.

The emission calculations given thus far apply to

[17] L. Oster, Phys. Rev. **116**, 474 (1959).
[18] H. Rosner, Report AFSWC-TR-58-47, Republic Aviation Coporation, Farmingdale, New York, 1958 (unpublished).
[19] S. Hayakawa, N. Hokkō, Y. Terashima, and T. Tsuneto, Paper P/1330, *Proceedings of the Second United Nations International Conference on the Peaceful Uses of Atomic Energy, Geneva, September 1958* (United Nations, Geneva, 1958), Vol. 32, p. 385.

plasmas with small optical depth τ, so that Eq. (1) gives $P(\omega)d\omega=(\frac{1}{2}kT_rSd\omega/2\pi\lambda^2)(\tau_1+\tau_2)$. For low absorption, but large plasma dimension L, so that the τ's are not small, we must use the full form of Eq. (1). The emission is there proportional to $1-e^{-\tau_n}$, so that a line spreading typical of optical spectra with large self-absorption is produced. A measure of the self-absorption is the optical depth at the line center, $\omega_p^2L/c\nu_c$, when α is given by Eq. (3) with $\theta=\pi/2$.

C. Emission from a Strongly Absorbing Plasma

When $(\alpha\lambda/4\pi)$ is not small, the full expressions for α, which are given by Mower,[11] must be used to obtain the emission. In a highly absorbing plasma, reflections that occur at the plasma boundaries will reduce the power radiated, as discussed in Sec. I. However, since the reflection coefficient will depend on the detailed geometry and environment of the plasma, we shall assume in the following discussion that the reflection coefficient has been measured separately and used to correct the emission values measured. Thus, we show in Fig. 5 the quantity $P(\omega)/[B(\omega)(1-\Gamma)]=1-e^{-\tau}$ for the resonant wave. Figure 5(a) is for $\theta=0$; Fig. 5(b) is for $\theta=\pi/2$. It is seen that the plasma radiates as a blackbody over bands of frequencies, and radiates much less outside of these bands, the magnitude outside depending in a more sensitive way upon (ν_c/ω) than the magnitude within them.

III. MEASUREMENTS OF THE EMISSION

A. Apparatus

The measurements of microwave radiation were performed on a 3000-Mc/sec Dicke radiometer[20] with a 2-Mc/sec bandwidth and a sensitivity of 10^{-17} w for a 1-sec integration time. The plasma under study was a section of the positive column of a dc hot-cathode discharge in helium. The discharge tube was placed axially along a tape-wound solenoid that produced the static magnetic field. The section of the positive column passed through a waveguide that could be arranged with its axis either along or perpendicular to the magnetic field; the electric vector in the waveguide (in the absence of a plasma) was maintained perpendicular to the magnetic field for both waveguide orientations. The magnetic field could be swept automatically and the radiometer output continually traced on a recorder. Since the radiation had a sharp spectral response (at cyclotron resonance, for example), a waveguide filter was inserted to suppress one of the two heterodyne sidebands.

Since the experiments were performed with bounded waves, the results of Sec. II, which are for plane waves, would not apply. However, for a weakly absorbing, tenuous plasma (which perturbs the waveguide fields only slightly), Eq. (2) can be applied with the result that Eqs. (3) and (4) are multiplied by $[1-(\lambda/\lambda_c)^2]^{-\frac{1}{2}}$,

[20] J. L. Hirshfield, Ph.D. thesis, Department of Physics, Massachusetts Institute of Technology, 1960 (unpublished).

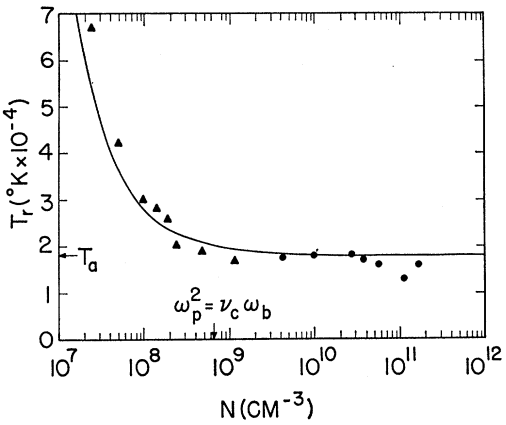

FIG. 6. Measurements of radiation temperature in helium. As a function of electron density N. ▲ Cyclotron radiation; ● blackbody radiation; —theory.

where λ_c is the waveguide wavelength for the mode considered. A complete solution for the absorption coefficient of a rectangular waveguide, even uniformly filled with plasma and immersed in a static magnetic field of arbitrary direction, has not been obtained, but two results[20] of the exact approach have been found: (1) For a tenuous plasma, the perturbation solution mentioned above is correct; (2) for a highly absorbing bounded plasma, the electron resonance appears at the same frequency as for an unbounded plasma, namely, $\omega^2=\omega_b^2+\omega_p^2\cos^2\theta$.

B. Measurements of Radiation Temperature

For any dependence of ν_c upon velocity, we can integrate Eq. (8) over all frequencies to obtain $P=(\omega_p^2\omega_b^2/3\pi c^3)[(1+\cos^2\theta)/2]\bar{u}_e$ w/m^3, where $\bar{u}_e=\frac{1}{2}\int_0^\infty mv^4f(v)dv$ is the average electron energy.

With $\theta=\pi/2$, values of $\bar{u}_e$ were obtained experimentally by graphically integrating the total power under resonance lines. Values of ω_p^2 were determined from tube current and electric field. Sample measurements taken at 0.037 mm Hg of helium pressure are shown in Fig. 6, in which we have plotted $T=2\bar{u}_e/3k$ against the electron density. Also shown are values of T_r obtained when the plasma radiates as a blackbody. The theoretical line is for the electron temperature in the discharge and is obtained by assuming its variation to be $T_e=T_aD_s/D_a$, where T_a is the observed value of T_e well within the ambipolar diffusion region (see horizontal arrow in Fig. 6), and D_s and D_a are the transitional and ambipolar diffusion coefficients, whose ratio is obtained from the results of Allis and Rose,[21] for an electron-to-ion mobility ratio of 32.

C. Measurements of Linewidth

When thermal effects do not influence the absorption coefficient, Eq. (8) gives the emission profile, whose

[21] W. P. Allis and D. J. Rose, Phys. Rev. **93**, 84 (1954).

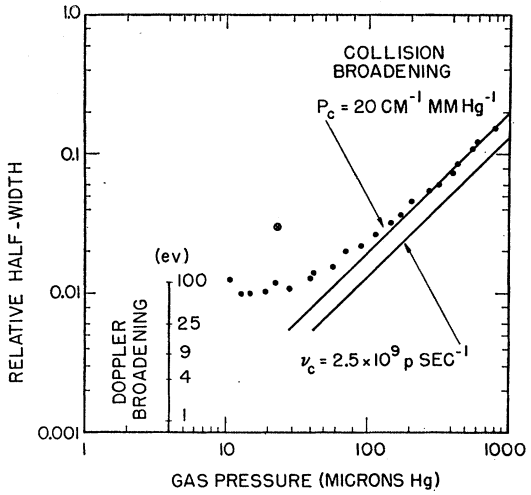

FIG. 7. Measurements of linewidth of cyclotron resonance radiation as a function of gas pressure.

half-width $\Delta\omega_{\frac{1}{2}}$ is related to $\nu_c(v)$; for ν_c=constant, $\Delta\omega_{\frac{1}{2}}=\nu_c$. For pure Doppler broadening, assuming a Maxwellian electron velocity distribution, we have $\Delta\omega_{\frac{1}{2}}=\omega_b(kT_e \ln 2/mc^2)^{\frac{1}{2}}$. In addition, inhomogeneities in the dc magnetic field and transit-time effects[22] can also influence the linewidth. Measurements of linewidth as a function of gas pressure for a fixed value of opacity at the line center, $\omega_p^2 L/c\nu_c=0.1$, are shown in Fig. 7. For comparison, two theoretical curves are shown: one for $\nu_c=2.5\times10^9 p_0$ sec^{-1}, an approximate value[23] in helium for electron energies greter than approximately 10 ev; and one for the probability of collision $P_c=\nu_c/p_0 v$ $=20$ cm^{-1} mm Hg^{-1}, the measured value[24] at room temperature which is approximately valid up to an energy equal to several electron volts. The second curve was obtained by evaluating Eq. (6), which is proportional to $\int_0^\infty [x^2 e^{-x}/(x+a)]dx$ for constant P_c, where $a=(m/2kT)[(\omega-\omega_b)/p_0 P_c]^2$; values of this integral have been tabulated by Dingle *et al.*[25] The half-width in this case is $\Delta\omega_{\frac{1}{2}}=7.50\times10^5 p_0 P_c T_e^{\frac{1}{2}}$, where T_e is in electron volts, and the curve shown in Fig. 7 is for $T_e=4$ ev. The fit between experiment and theory is seen to favor this second case.

The data in Fig. 7 are seen to depart radically from either of the cases mentioned above at low pressures. The departures can be explained qualitatively by either Doppler broadening or magnetic-field inhomogeneities. Estimates of the effects of Doppler broadening can be made by referring to the scale inserted in Fig. 7, which gives the half-widths for pure Doppler broadening corresponding to the values of T_e shown. The effects of inhomogeneous magnetic field were demonstrated by purposely making the field nonuniform; this produces a considerably wider emission line, as shown by the point marked ⊗ in Fig. 7. The strong deviations from collision broadening at low pressures probably result from some combination of Doppler and inhomogeneous magnetic-field effects.

D. Measurements of Line Shape

In order to avoid any influence of electron transit through the receiving aperture on the emission profile, the plasma occupied a length in the receiving waveguide of 23 cm. This was accomplished by offsetting the waveguide to permit the discharge-tube electrodes to be sufficiently far from the interaction region. Furthermore, the magnetic field was made uniform (better than 0.5% over the plasma volume) by inserting iron shims in the solenoid interior. Figure 8 shows a typical experimental profile (labeled $\beta=\infty$) at high pressure, $p=0.190$ mm Hg; here collision broadening is expected to dominate the profile. For comparison, theoretical Lorentz profiles for constant ν_c and for constant P_c are also shown, as solid and dashed lines, respectively. Note that the data do not apply to one case more than to the other.

At lower pressures, where Doppler broadening is expected to enter in, the experimentally determined

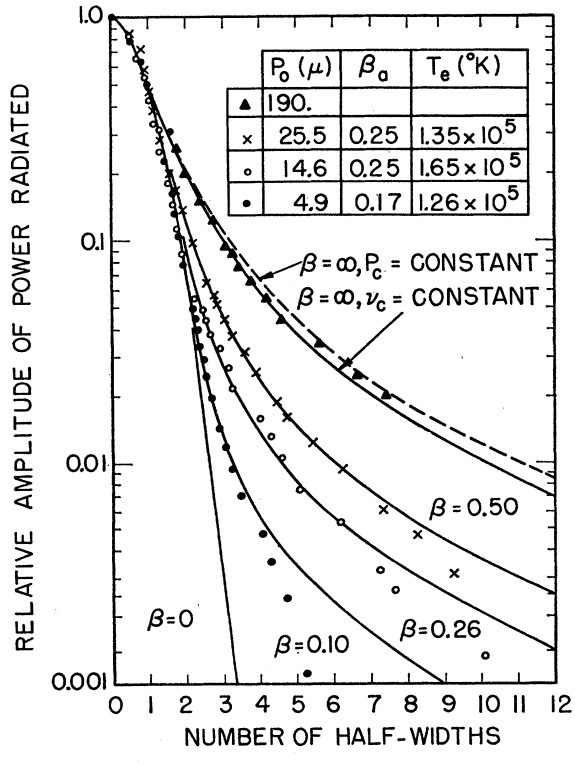

FIG. 8. Line profiles of cyclotron resonance radiation.

[22] S. Gruber, Quarterly Progress Report No. 58, Research Laboratory of Electronics, Massachusetts Institute of Technology, July 15, 1960 (unpublished), pp. 14–17.
[23] S. C. Brown, *Basic Data of Plasma Physics* (Technology Press of Massachusetts Institute of Technology, Cambridge, Massachusetts, and John Wiley & Sons, Inc., New York, 1959), p. 54.
[24] J. L. Hirshfield and S. C. Brown, J. Appl. Phys. **29**, 1749 (1958).
[25] R. B. Dingle, Doreen Arndt, and S. K. Roy, Appl. Sci. Research **B6**, 144–252 (1956).

profiles are also shown in Fig. 8, together with the theoretical best fits.[16] Significant are the large differences between Voigt profiles for $0<\beta<\infty$; for $\beta=0$ the profile is approximately two orders of magnitude lower than that for $\beta=\infty$, at three half-widths. Here $\beta=c\nu_c/v_t\omega$ is proportional to the ratio of collision to Doppler half-widths, if each contributes separately. The insert in Fig. 8 shows the values of pressure at which the experiments were obtained and values of electron temperature inferred from obtaining the best fit between experiment and theory. The parameter β_a listed in the insert of Fig. 8 is inferred from independent measurements of the plasma opacity at the line center.[15] Knowledge of this was necessary in order to correct the line profiles for self-absorption.

The experimental deviations from theory below a relative amplitude of 10^{-2} in Fig. 8 are significant. These could be caused by depletion in the tail of the electron velocity distribution, which has been assumed to be Maxwellian.

E. Emission from Highly Absorbing Plasmas

Our measurements of radiation from highly absorbing plasmas [$(\alpha\lambda/4\pi)$ not negligible compared with unity] are not amenable to comparison with the theory of Sec. II-C because the experiments were for bounded inhomogeneous plasmas, and the theory is for unbounded homogeneous plasmas. Nevertheless, some characteristics of the observed emission follow the qualitative predictions of theory, as shown in Fig. 9 in which we have reproduced radiometer output recorder traces for various values of $(\omega_p/\omega)^2$. Here $p_0=0.051$ mm Hg, and $\theta=\pi/2$. The pronounced asymmetrical broadening is evident in the direction of lower magnetic field as one goes to higher values of $(\omega_p/\omega)^2$; also evident is the shifting of the peaks of the resonance profile toward lower magnetic fields. The flattening of the peaks for the higher values of $(\omega_p/\omega)^2$ results from large values of the optical depth τ, brought about here by large values of α, in contrast to Fig. 8 in which τ was large because of a large plasma size. In the experiment leading to Fig. 9, $4\pi L/\lambda=1.25$.

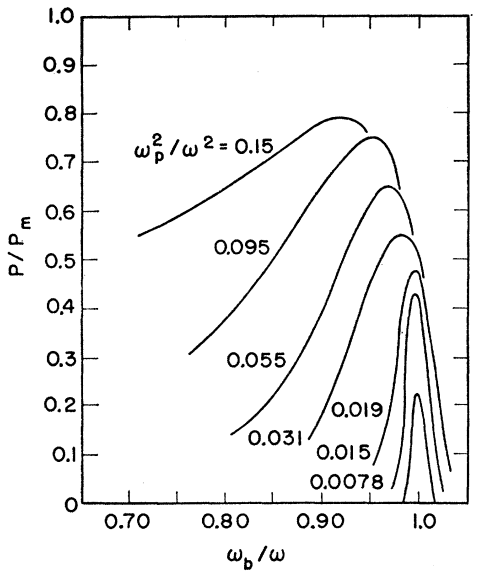

FIG. 9. Radiation from a nontransparent plasma.

ACKNOWLEDGMENTS

The authors acknowledge many helpful discussions with Dr. George Bekefi during the course of this work, and the invaluable technical assistance of John J. McCarthy, both of the Research Laboratory of Electronics, M. I. T. Computations leading to Figs. 3, 4, and 5 were performed by the Computation Center, M. I. T.